PROCEEDINGS OF SCIENCE

Searches for squarks and gluinos in fully hadronic final states with the ATLAS detector

David W. Miller[*†]
University of Chicago and the Enrico Fermi Institute
E-mail: David.W.Miller@uchicago.edu

Despite the absence of experimental evidence, weak scale supersymmetry remains one of the best motivated and studied Standard Model extensions. The recent increase in the center of mass energy of the proton-proton collisions gives a unique opportunity to extend the sensitivity to production of supersymmetric particles at the Large Hadron Collider. We present results of two searches for squarks and gluinos using fully hadronic final states at $\sqrt{s} = 13$ TeV with >10 fb^{-1} of 2016 data collected by the ATLAS detector. These searches use three primary classes of event selection observables, including novel Recursive Jigsaw and Lorentz-boosted object reconstruction approaches.

38th International Conference on High Energy Physics
3-10 August 2016
Chicago, USA

[*]Speaker.
[†]On behalf of the ATLAS Collaboration.

PoS(ICHEP2016)112

1. Introduction

The increase of the center-of-mass energy of the Large Hadron Collider (LHC) from $\sqrt{s} = 8 \to 13$ TeV between 2012 and 2015 has brought with it significant increases in sensitivity to strongly produced new physics, such as the production of Supersymmetric (SUSY) gluino ($\tilde{g}$) and squark ($\tilde{q}$) pairs. The accumulation of additional integrated luminosity between 2015 and 2016 has further extended the reach of searches for these final states. These proceedings report on the results from the ATLAS Experiment [1] from two approaches to searching for squark and gluino-initiated processes that yield final states dominated by jets and missing transverse energy ($E_{\mathrm{T}}^{\mathrm{miss}}$).

The analysis described in Sec. 2.1 is optimized for the discovery of squark and gluino-initiated processes that yield final states with 2–6 jets and significant $E_{\mathrm{T}}^{\mathrm{miss}}$ due to the escape of the lightest supersymmetric particle, assumed to be the neutralino ($\tilde{\chi}_1^0$), as shown in Fig. 1(a). This search is conducted using both a traditional selection procedure based on the effective mass (M_{eff}), referred to as the "M_{eff}-based approach," as well as using the Recursive Jigsaw Reconstruction (RJR) [2], referred to as the "RJR-based approach" [3].

Since the top quark plays an important role in new physics scenarios, the analysis described in Sec. 2.2 is optimized for the case in which pair-produced gluinos each decay to two top quarks via intermediate off-shell stop squarks, as shown in Fig. 1(b). Multiple b-quarks are thus expected in the final state. The sensitivity to high-mass gluinos necessitates the use of observables that can distinguish final states with Lorentz-boosted top quarks [4].

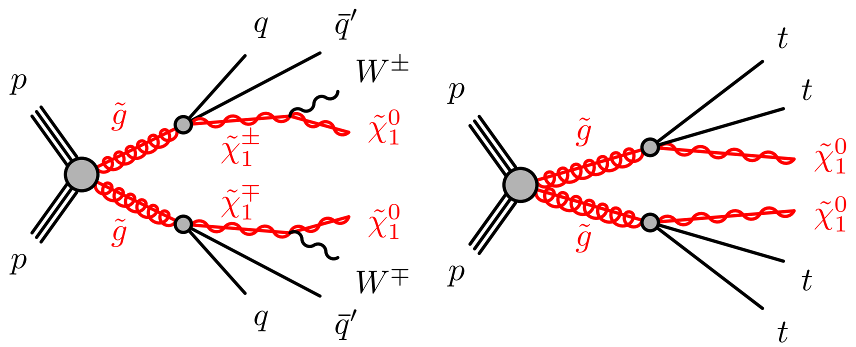

(a) Glunio one-step decay via charginos, $\tilde{\chi}_1^{\pm}$ (b) Gluino-mediated stop production

Figure 1: Examples of the processes targeted by the (a) jets+$E_{\mathrm{T}}^{\mathrm{miss}}$ analysis (both the M_{eff}-based and RJR-based approaches) and the (b) multi-b analysis.

2. Fully hadronic SUSY searches

Each of the analyses presented uses selections on various observables to enhance signals relative to the Standard Model (SM) background. Signal regions (SRs) are defined using Monte Carlo (MC) simulation of the signal processes and the SM backgrounds, control regions (CRs) are used to estimate those backgrounds, and validation regions (VRs) are used to test the descriptions that those estimates provide.

Observables optimized for SUSY searches cover three primary categories (see Table 1) [5]: *missing energy-type*, *energy scale-type*, and *energy structure-type*. These yield information about

PoS(ICHEP2016)112

the properties of invisible states, the overall energy or mass scale of the event, and the distribution of the visible energy throughout the event, respectively. Table 1 defines the primary observables used in the searches described in these proceedings, as well as the category into which they fall according this classification.

Table 1: Categories and definitions of observables used in SUSY searches. For more information see Refs. [3,4].

Category	Observable	Definition
Missing energy-type	Missing transverse momentum	$E_{\mathrm{T}}^{\mathrm{miss}}$ and $\vec{p}_{\mathrm{T}}^{\,\mathrm{miss}}$
	$E_{\mathrm{T}}^{\mathrm{miss}}$ significance	$E_{\mathrm{T}}^{\mathrm{miss}}/\sqrt{H_{\mathrm{T}}}$
	RJR H-scale for 1 visible, 1 invisible state	$H_{1,1}^{\mathrm{PP}}$ *(similar to E_T^{miss})*
Energy scale-type	Scalar sum of visible momenta	$H_{\mathrm{T}} = \sum_{\mathrm{jets}} p_{\mathrm{T}}$ *(also with 4 high p_T jets)*
	Effective mass	$M_{\mathrm{eff}} = \sum_{\mathrm{jets}} p_{\mathrm{T}} + \sum_{\mathrm{leptons}} p_{\mathrm{T}} + E_{\mathrm{T}}^{\mathrm{miss}}$
	Transverse mass	$m_{\mathrm{T}} = \sqrt{2 p_{\mathrm{T}}^{\ell} E_{\mathrm{T}}^{\mathrm{miss}} (1 - \cos(\Delta\phi(\vec{p}_{\mathrm{T}}^{\,\mathrm{miss}}, \ell))}$
	RJR H-scale	$H_{2,1}^{\mathrm{PP}}$, $H_{4,1}^{\mathrm{PP}}$
	RJR p_{T} scales	$p_{TS}^{\mathrm{CM}}, p_{TS}^{\mathrm{ISR}}$ *(total p_T of CM or ISR jets)*
Energy structure-type	Jet multiplicity	N_{jet}, $N_{b-\mathrm{jet}}$
	Total jet mass	$M_{\mathrm{J}}^{\Sigma} = \sum m^{\mathrm{jet}}$ *(using large-radius jets)*
	Angular distributions	$\Delta\phi_{\mathrm{min}}^{4j} = \min(\lvert\phi_{\mathrm{any-jet}} - \vec{p}_{\mathrm{T}}^{\,\mathrm{miss}}\rvert) > 0.4$
	Aplanarity	$A = (3/2)\lambda_3$
	RJR QCD $E_{\mathrm{T}}^{\mathrm{miss}}$ alignment	Δ_{QCD}

2.1 Zero-lepton final states with 2–6 jets

This analysis uses both M_{eff}-based and RJR-based approaches to searching for SUSY. Any event with an electron or muon with $p_{\mathrm{T}} > 10$ GeV or no jet with $p_{\mathrm{T}} > 50$ GeV is vetoed. In the case of the M_{eff}-based search, the final signal selection uses requirements on both M_{eff}, which sums over all jets with $pT > 50$ GeV and $E_{\mathrm{T}}^{\mathrm{miss}}$, which is independently required to be larger than 250 GeV. The RJR-based search uses primarily $H_{1,1}^{\mathrm{PP}}$ and either $H_{2,1}^{\mathrm{PP}}$ (for squark-pair production) or $H_{4,1}^{\mathrm{PP}}$ (for gluino production) with additional selections placed on dimensionless quantities for further background suppression and signal discrimination. These observables are described in much more detail in Ref. [3].

Specific CRs are defined for estimating backgrounds from multi-jets, $Z(\to \nu\nu)$+jets, $W(\to \ell\nu)$+jets and $t\bar{t}$. Fig. 2 shows the estimates for $Z(\to \nu\nu)$+jets and $t\bar{t}$ for the RJR and M_{eff}-based approaches, respectively. The $Z(\to \nu\nu)$+jets background is estimated using a sample of γ+jets events with $p_{\mathrm{T}}(\gamma) > 150$ GeV in which the photon is treated as invisible in the $E_{\mathrm{T}}^{\mathrm{miss}}$ calculation. The $t\bar{t}$ background is estimated using a b-tagged single lepton sample with a low m_{T} selection.

Systematic uncertainties are primarily due to background predictions in the signal regions and from the MC simulation modeling of minor backgrounds. The overall background uncertainties range from 8% to 43% across the various signal regions.

PoS(ICHEP2016)112

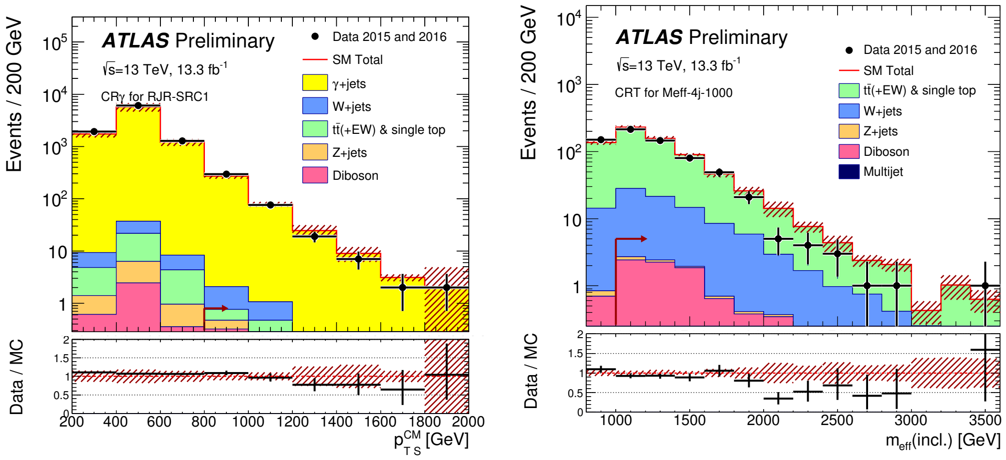

(a) $Z(\rightarrow \nu\nu)$+jets control region (b) Top pair production control region

Figure 2: Control regions for (a) $Z(\rightarrow \nu\nu)$+jets in the RJR-based search and (b) $t\bar{t}$ in the $M_{\rm eff}$-based search [3].

The results are shown in Fig. 3 with a comparison of the observed and expected SM event yields as a function of signal region in the two approaches. The most significant observed excess across the thirty signal regions for both searches occurs in SR Meff-6j-1800. In this case, background-only hypothesis has a p-value of 0.01, corresponding to a significance of 1.56 standard deviations. Following these null results, limits are set on the allowed combinations of $\tilde{\chi}_1^0$ mass and $\tilde{g}$ mass, as shown in Fig. 4. Additional interpretations can be found in Ref. [3].

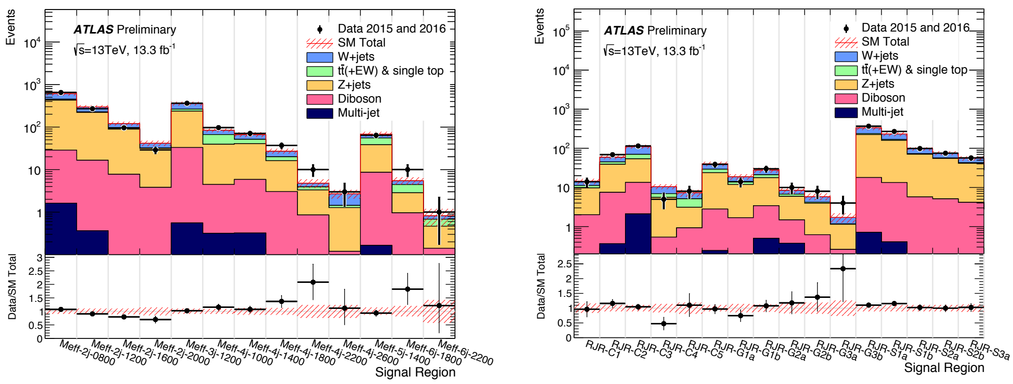

(a) $M_{\rm eff}$-based search (b) RJR-based search

Figure 3: Comparison of the observed and expected event yields as a function of signal region in the (a) Meff-based and (b) RJR-based approaches [3].

2.2 Multi-b final states

This analysis uses selections that require large jet and b-jet multiplicities to search for SUSY that predominantly decays to heavy flavor final states, with at least three jets identified as b-jets. Several signal regions are designed to cover different ranges of gluino and $\tilde{\chi}_1^0$ masses. For models

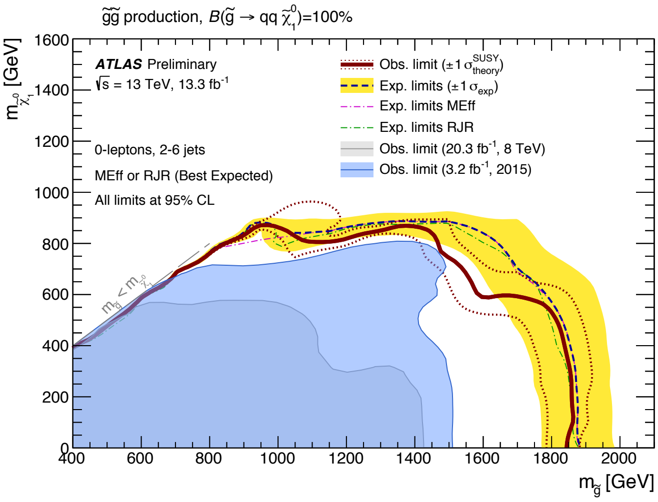

Figure 4: Exclusion limits for direct production of gluino pairs with decoupled squarks. Exclusion limits are obtained by using the signal region with the best expected sensitivity at each point. Expected limits from the Meff- and RJR-based searches separately are also shown for comparison. The blue dashed lines show the expected limits at 95% CL, with the light (yellow) bands indicating the 1σ excursions due to experimental and background-only theoretical uncertainties [3].

with multiple tops in the final state and large mass differences between the gluino and $\tilde{\chi}_1^0$, the top quarks can be highly boosted and their decay products collimated. A topological observable built from the sum of the masses of large-radius jets, the total jet mass (M_J^Σ), is used to enhance the signal discrimination in these regions.

Fig. 5 shows the distribution of $m_{T,\text{min}}^{b\text{-jets}}$ and M_J^Σ after a preselection that requires $E_T^{\text{miss}} >$ 200 GeV, $N_{\text{jet}} > 4$, $N_{b-\text{jet}} > 2$, and $\Delta\phi_{\text{min}}^{4j} > 0.4$. The transverse mass $m_{T,\text{min}}^{b\text{-jets}}$ is related to m_T by the replacement of the lepton by a b-jet. The signal regions further select events with large $m_{T,\text{min}}^{b\text{-jets}} > 80$ GeV, $E_T^{\text{miss}} > 300-450$ GeV and $M_{\text{eff}} > 1$ TeV or higher.

Background estimation is focused on $t\bar{t}$ events with addition high-p_T b-jets jets. For each signal region, the $t\bar{t}$ background is normalized in a dedicated control region. The predicted and observed event yields are shown in Fig. 6(a), where no significant excess is found. Exclusion limits in the $\tilde{\chi}_1^0$ and $\tilde{g}$ mass plane for the gluino-mediated stop model are thus determined, as shown in Fig. 6(b). Additional interpretations can be found in Ref. [4].

3. Summary and conclusions

ATLAS has a robust and broad effort devoted to searching for SUSY in fully hadronic final states, using new techniques, novel approaches to final state reconstruction, and a holistic perspective on using various classes of observables for these searches. The flagship jets+E_T^{miss} search is presented with the first 2016 data and significantly extended the Run 1 and 2015 sensitivity. The novel recursive jigsaw reconstruction technique for partitioning final state kinematics and constructing a dynamic and discriminating basis of event-level observables is shown for the first time. The dedicated search for $4b$ and 4 top SUSY processes using the total jet mass observable is also presented and demonstrates significantly extended sensitivity to natural SUSY.

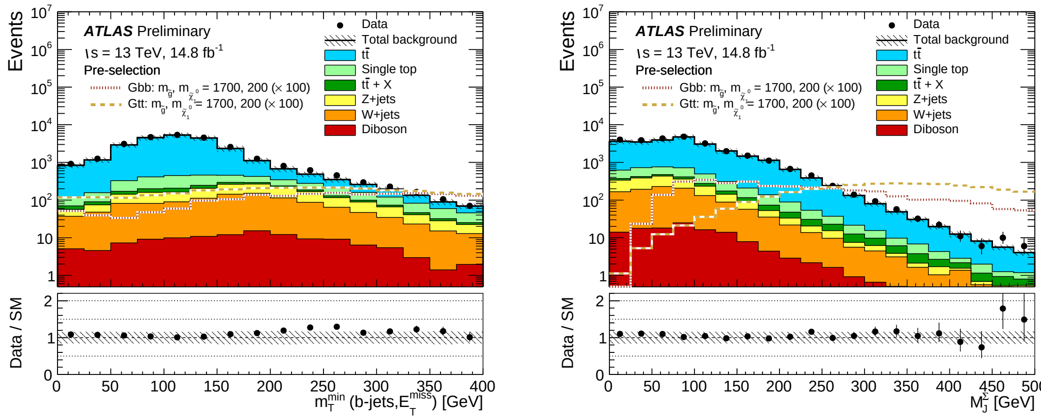

(a) Transverse mass using b-jets, $m_{\mathrm{T,min}}^{b\text{-jets}}$

(b) Total jet mass, M_J^{Σ}

Figure 5: Distributions of kinematic variables after preselection requirements for (a) $m_{\mathrm{T,min}}^{b\text{-jets}}$ and (b) M_J^{Σ}. The statistical and experimental systematic uncertainties are included in the uncertainty band. The lower part of each figure shows the ratio of data to the background prediction. All backgrounds are normalized using the best available theoretical calculation [4].

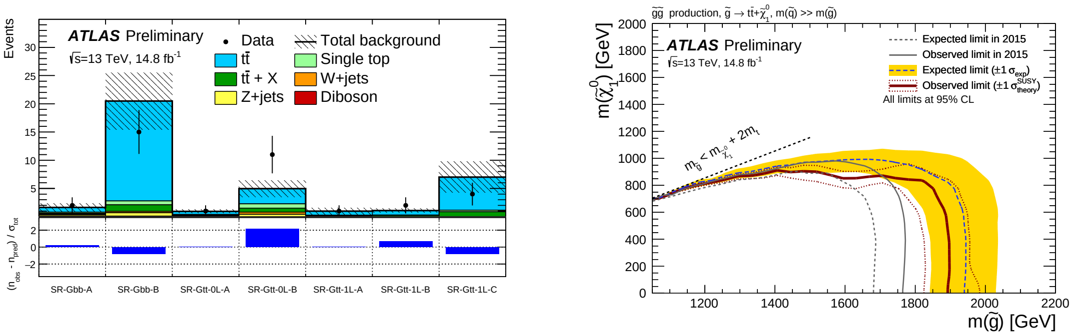

(a) Signal yields for each signal region

(b) Limits for gluino-mediated stop model

Figure 6: (a) Observed number of events and the predicted background yield in each signal region. The lower panel shows the pulls in each signal region. (b) Exclusion limits in the $\tilde{\chi}_1^0$ and $\tilde{g}$ mass plane for the gluino-mediated stop model. The dashed and solid bold lines show the 95% CL expected and observed limits, respectively. The shaded bands around the expected limits show the impact of the experimental and background theoretical uncertainties [4].

References

[1] ATLAS Collaboration, *The ATLAS Experiment at the CERN Large Hadron Collider*, JINST **3** (2008) S08003.

[2] P. Jackson, C. Rogan, and M. Santoni, *Sparticles in Motion - getting to the line in compressed scenarios with the Recursive Jigsaw Reconstruction*, arXiv:1607.08307 [hep-ph].

[3] ATLAS Collaboration, *Further searches for squarks and gluinos in final states with jets and missing transverse momentum at $\sqrt{s} = 13$ TeV with the ATLAS detector*, ATLAS-CONF-2016-078, 2016, https://cds.cern.ch/record/2206252.

[4] ATLAS Collaboration, *Search for pair production of gluinos decaying via top or bottom squarks in events with b-jets and large missing transverse momentum in pp collisions at* $\sqrt{s} = 13$ *TeV with the ATLAS detector*, ATLAS-CONF-2016-052, 2016, https://cds.cern.ch/record/2206134.

[5] T. Cohen, M. J. Dolan, S. El Hedri, J. Hirschauer, N. Tran, and A. Whitbeck, *Dissecting Jets and Missing Energy Searches Using n-body Extended Simplified Models*, JHEP **08** (2016) 038, arXiv:1605.01416 [hep-ph].